

## Chapter 5 Quadrupole Sources

### 5.1 The Mathematical Model

The basic wave equation for the quadrupole includes dependence on all three directions

$$\begin{aligned} \frac{1}{r^2} \frac{\partial}{\partial r} \left( r^2 \frac{\partial \phi}{\partial r} \right) + \frac{1}{r^2 \sin \theta} \frac{\partial}{\partial \theta} \left( \sin \theta \frac{\partial \phi}{\partial \theta} \right) + \frac{1}{r^2 \sin^2 \theta} \frac{\partial^2 \phi}{\partial \psi^2} - \frac{1}{c_0^2} \frac{\partial^2}{\partial t^2} (r\phi) &= 0 \\ \frac{1}{r^2} \frac{\partial}{\partial r} \left( r^2 \frac{\partial \Phi}{\partial r} \right) + \frac{1}{r^2 \sin \theta} \frac{\partial}{\partial \theta} \left( \sin \theta \frac{\partial \Phi}{\partial \theta} \right) + \frac{1}{r^2 \sin^2 \theta} \frac{\partial^2 \Phi}{\partial \psi^2} + k^2 \Phi &= 0 \end{aligned} \quad (5.1)$$

$\phi(\mathbf{r}, \theta, \psi, t)$  and  $\Phi(\mathbf{r}, \theta, \psi, \omega)$  are the velocity potentials. Both polar angles need to be taken into account for this case. The key physical variables are

$$\begin{aligned} p(r, \theta, \psi, t) &= \rho_0 \frac{\partial \phi}{\partial t} & u_\theta(r, \theta, \psi, t) &= -\frac{1}{r} \frac{\partial \phi}{\partial \theta} \\ u_r(r, \theta, \psi, t) &= -\frac{\partial \phi}{\partial r} & u_\psi(r, \theta, \psi, t) &= -\frac{1}{r \sin \theta} \frac{\partial \phi}{\partial \psi} \end{aligned} \quad (5.2)$$

#### 5.1.1 The Quadrupole as a Merging of Two Dipoles

The monopole in Chapter 3 had no preferred direction (the source was scalar). The dipole in Chapter 4 was the joining of two monopoles of opposite sign oriented along the z axis. The source was a force vector in that direction. The next step is the joining of two dipoles of opposite sign. Since we are dealing with two vectors, they can be oriented arbitrarily with respect to each other. When they are, the source is called an *oblique quadrupole*. Such a source can be resolved into two perpendicular components. One is called a *lateral quadrupole* where the orientation of one axis is perpendicular to the other. The second is called a *longitudinal quadrupole* where both axes are parallel {1.3}. In fluids, the lateral quadrupole is associated with shear flows and most studies suggest that it is this form that predominates in the sound generated.

### 5.2 The Single Frequency Point Lateral Quadrupole

#### 5.2.1 Physical Variables

For this case, one axis is perpendicular to the other. The velocity potential is

$$\phi_{lat} = \frac{Q_{lat}}{4\pi} \left[ \frac{3(1+ikr) - k^2 r^2}{r^3} \right] e^{i(\omega t - kr)} \cos \theta \cos \psi \quad (5.3)$$

Knowing that the dimensions of the velocity potential must be  $L^2/T$ , the dimensions of the quadrupole source strength must be  $L^5/T$ . The physical interpretation can be clarified best by first developing the two significant physical variables. Using the basic equations for these variables {A.3.2}, they are

$$p = \frac{ikZ_0Q_{lat}}{4\pi} \left[ \frac{3(1+ikr) - k^2r^2}{r^3} \right] e^{i(\omega t - kr)} \cos \theta \cos \psi$$

$$u_r = \frac{Q_{lat}}{4\pi} \left[ \frac{9(1+ikr) - 4k^2r^2 - ik^3r^3}{r^4} \right] e^{i(\omega t - kr)} \cos \theta \cos \psi$$
(5.4)

The other velocity components can be determined by carrying out the differentiations indicated in Eqs. 5.2.

### 5.2.2 Near Field

With  $kr \ll 1$ , both sound pressure and radial velocity increase with high powers of radius. This suggests that quadrupole action is much more “near field” than the lower order sources as shown in the equations to the right..

$$p = \frac{i3kZ_0Q_{lat}}{4\pi r^3} e^{i(\omega t - kr)} \cos \theta \cos \psi$$

$$u_r = \frac{9Q_{lat}}{4\pi r^4} e^{i(\omega t - kr)} \cos \theta \cos \psi$$

### 5.2.3 Far Field

The sound pressure and radial velocity decrease inversely with increasing radius. When  $kr \gg 1$ , the equations reduce to those shown on the right.

$$p = \frac{-ik^3Z_0Q_{lat}}{4\pi r} e^{i(\omega t - kr)} \cos \theta \cos \psi$$

$$u_r = \frac{-ik^3Q_{lat}}{4\pi r} e^{i(\omega t - kr)} \cos \theta \cos \psi$$

### 5.2.4 Radiation Impedance

The expression for radial acoustic impedance is complicated for arbitrary distances from the source; it is given in Eq. 5.5 and is shown graphically in Figure 5-1. The figure clearly shows how large the reactive impedance is with respect to the sound (resistive) part at close distances. Quadrupole impedance is compared with the impedance of the lower order sources in {6.2}.

$$Z_r = \frac{k^6r^6 + i(27kr + 6k^3r^3 + k^5r^5)}{81 + 9k^2r^2 - 2k^4r^4 + k^6r^6} Z_0$$
(5.5)

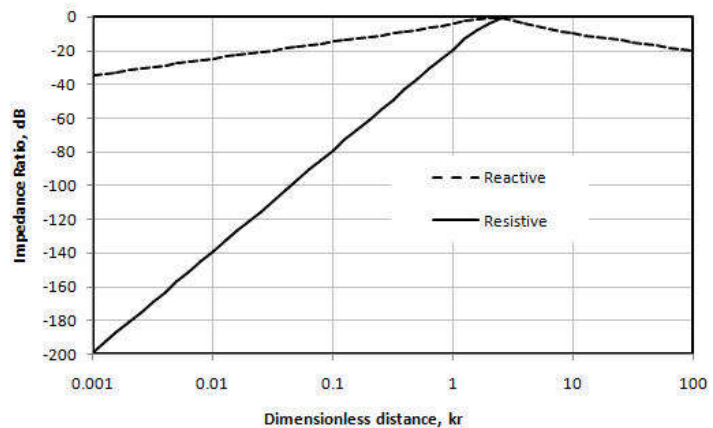


Fig. 5-1 The radial impedance of a lateral quadrupole.

### 5.2.5 Sound Intensity

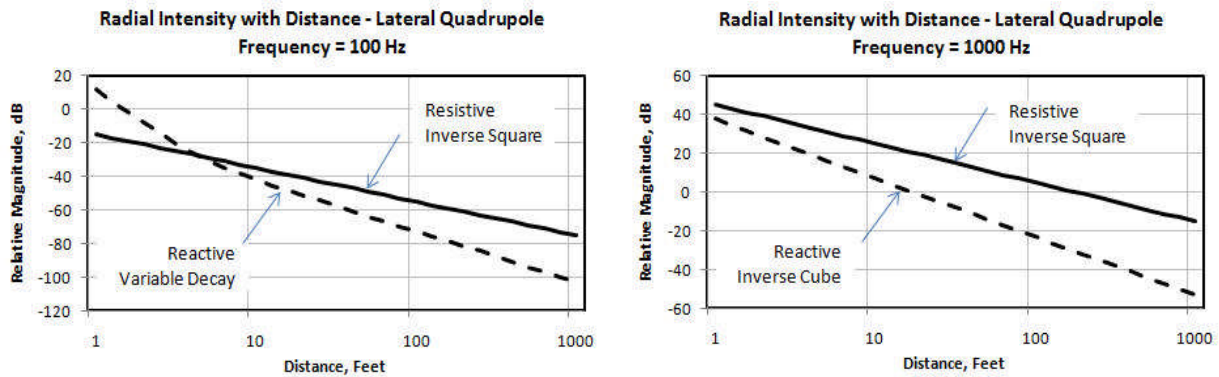
The radial intensity is

$$I_r(r, \theta, \psi) = \frac{Q_{lat}^2 Z_0}{16\pi^2} \left[ \frac{k^6 r^6 + ikr(27 + 6k^2 r^2 + k^4 r^4)}{r^8} \right] \cos^2 \theta \cos^2 \psi \quad (5.6)$$

$$I_r(r, \theta, \psi) = \frac{k^6 Q_{lat}^2 Z_0}{16\pi^2 r^2} \cos^2 \theta \cos^2 \psi$$

The second equation is the far sound field approximation for  $kr \gg 1$ . The resistive component of the radial intensity increases with a high power of the frequency. The reactive component of the radial intensity is considerably larger at low frequencies suggesting more incompressible flow components than the dipole or monopole source. The other components of intensity are totally reactive creating a fluid loading of the source; they have a complex dependence on angle.

The change in the resistive and reactive components (the bracketed term in Eqs. 5.6) of the radial intensity with distance and frequency is shown in Figures 5-2 and 5-3.



*Figs. 5-2 and 5-3 Radial impedance of a lateral quadrupole at two frequencies.*

The resistive impedance decays with the square of distance while the reactive impedance decays rapidly and then with the cube of distance. Note that at low frequencies and close-in distances, the sound field is buried in the reactive (hydrodynamic) motion. The directivity of the source is considerably more complicated than for the lower order sources. This latter comment is based on one source that is fixed in space. In fluid flows neither of these conditions apply, so directivity information is not helpful {5.5.1}. If the source does meet the conditions, the complexity of the sound field can easily separate it from dipole or monopoles.

**Key Point:** Point lateral quadrupoles are inefficient sources of sound compared with the lower order sources and have more complex sound field directivity..

### 5.2.6 Estimates of Sound Intensity

The estimated sound intensity is given in the first of Eqs. 5.7. The ratio of the sound intensity estimate to the actual (real) part of the radial intensity is given in the second equation.

A graph of the ratio is shown in Figure 5-4. The error exceeds 1 dB when  $kr$  is less than 4. This is a greater error restriction than for the dipole source. The error can be quite significant

$$EST[I_r] = \frac{p \bullet p^*}{Z_0} = \frac{Z_0 Q_{lat}^2}{16\pi^2} \left[ \frac{9k^2 r^2 + 3k^4 r^4 + k^6 r^6}{r^8} \right] \sin^2 \theta \cos^2 \psi \quad Ratio = \frac{9 + 3k^2 r^2 + k^4 r^4}{k^4 r^4} \quad (5.7)$$

when close to the source. For example the minimum distance is 137 inches at 63 Hz, and 34 inches at 250 Hz.

Since the range of the near field is greater at low frequencies, spectrum distortion occurs if the measurement is made too close to the source.

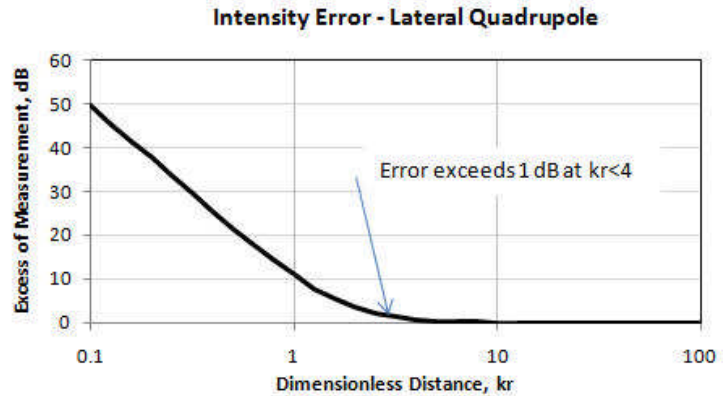


Fig. 5-4. The error in estimating lateral quadrupole sound intensity from sound pressure measurements.

### 5.2.7 Sound Power

Integrating the far field radial intensity over the surrounding volume yields Eq. 5.8

$$W_{lat} = \frac{k^6 Q_{lat}^2 Z_0}{24\pi} \quad (5.8)$$

This relationship implies that the sound power increases with the *sixth* power of the frequency *forever!* Aside from the restriction that the source is a point, does this dependence make sense? The quantity  $Q_{lat}$  is convenient mathematically, but has little physical significance. This needs to be corrected.

### 5.2.8 Source Strength Interpretation

Look for any monopole component (volumetric flow rate). The result of integrating the radial velocity is

$$Q_{lat} = \int_0^{2\pi} \int_0^{\pi} u_r r^2 \sin \theta d\theta d\psi = 0$$

The  $\psi$  integral is zero so  $Q_{lat}$  is not a volumetric flow rate as might be surmised from its dimensions  $L^5/T$ .

Look for any dipole component (net force acting on the medium). The differential forces are

$$\begin{aligned} dF_z &= pr^2 \cos \theta \sin \theta d\theta d\psi \\ dF_x &= pr^2 \sin^2 \theta \cos \psi d\theta d\psi \\ dF_y &= pr^2 \sin^2 \theta \sin \psi d\theta d\psi \end{aligned}$$

When the angular dependence of the sound pressure is added to these terms and the integration performed, each integral equals zero. There is *no net force* acting the medium.

For the monopole, the source was scalar (no preferred direction), and for the dipole, the source vector (one preferred direction). The quadrupole is another order higher (two preferred directions), a second order tensor. Applied stress has this property. Figure 1-5 in Chapter 1 shows that two opposing forces displaced laterally make a shear moment resulting in a lateral quadrupole. The geometry of that figure suggests that one preferred direction  $\mathbf{z}$  is in the direction of the opposing forces and the second direction  $\mathbf{x}$  is perpendicular to it. For that the tensor symbol  $\tau_{xz}$  will be used. To calculate the moment created by the forces, convert the  $\mathbf{z}$  coordinate to polar coordinates, use the differential forces given above and perform a spatial integration of the moment arm close to the source. When this is carried out, the source  $\mathbf{Q}_{lat}$  ( $\mathbf{L}^5/\mathbf{T}$ ) is replaced by  $\tau_{xz}$  ( $\mathbf{FL}$ ) and the far sound field equations become

$$I_r(r, \theta, \psi) = C_1 \frac{k^4 \tau_{xz}^2}{Z_0 r^2} \cos^2 \theta \cos^2 \psi \quad (5.9)$$

$$W_{lat} = C_2 \frac{k^4 \tau_{xz}^2}{Z_0}$$

The  $\mathbf{C}$  values are constants and are not pertinent to the development. By analogy to Eq. 3.5 for the monopole and Eq. 4.7 for the dipole, the sound power of the lateral quadrupole can be expressed in the form below.

$$W_{lat} = \frac{C_3}{Z_0 c_0^4} \left( \overline{\frac{\partial \dot{\tau}_{xz}}{\partial t}} \right)^2 \quad (5.10)$$

***The sound from a lateral quadrupole is created by the mean square of the time rate of change of the shear stress rate.***

### 5.2.9 Dimensional Analysis

By introducing dimensionless factors into the sound power equation, it becomes

$$\begin{aligned} W_{lat} &= \frac{K \rho_0}{c_0^5} \widehat{\tau}_{xz}^2 S^4 U^8 L^2 \\ \widehat{W}_{lat} &= K \widehat{\tau}_{xz}^2 S^4 M^5 \end{aligned} \quad (5.11)$$

See {A.2.2} for definitions of the dimensionless ratios. This equation applies for point-like lateral quadrupoles. This is the well known  $\mathbf{U}^8$  law for jet noise. Because of the high

exponent on the Strouhal Number, if it depends on Reynolds number, the  $U^8$  speed law may not be achieved, {6.4.2}. A similar caution applies to the shear moment.

**Key Points:** The dependence of the point lateral quadrupole on frequency and speed is considerably higher than for the monopole or dipole, suggesting this source is important at higher frequencies and speeds. No derivation for the finite lateral quadrupole is given, since there is little evidence that finite size effects are important in the major application of this source: jet noise.

### 5.3 The Single Frequency Point Longitudinal Quadrupole

The development of the longitudinal quadrupole is unnecessary for this monograph since it appears that it is not an important factor in high speed flows. The primary features of this quadrupole is that it has a more complex near field, and the intensity has a  $\cos^4 \theta$  directivity. The form for the sound power (Eqs. 5-9, 5.11) is the same as that for the lateral quadrupole. However, the constant is a factor of three greater than  $C_2$  for the lateral quadrupole.

### 5.4 Modeling Quadrupoles

The basic feature of the theoretical quadrupole is a highly directional sound field resulting from stresses being applied to the surrounding fluid. Some real sources may meet these requirements but others do not, so may be described only as *quadrupole-like*.

1. *Fluctuating stresses in free space.* They create a multi-directional sound field.
2. *Fluctuating stresses along a surface.* The orientation of the stresses determine their interaction with the reflected image source.

The stresses are related to fluctuations in the local momentum flux. Generally, the only significant quadrupole sources are those generated by turbulent fluid flows. The size of turbulent eddies appears to be quite small relative to the wavelength of the sound generated by them, so the sound power equation developed based on a point source (Eq. 5.11) has been verified experimentally [12, 13]. The difficulty in applying quadrupole concepts to determine sound field directivity is that the turbulent eddy structure is randomly oriented and embedded in a high speed flow with large velocity gradients that cause refraction.

### 5.5 Modeling Category I Quadrupole Sources

#### 5.5.1 Subsonic Jets

The theoretical models have each of their axes in a defined direction, so one would expect to be able to measure source directivity. Unfortunately, not many higher order sources have such fixed directivity. The initial interest in these sources was in the noise from jet engines that was determined to be of quadrupole nature. The flow from a subsonic jet is highly turbulent, so the source orientations are more nearly random; one cannot expect to derive any information about the source from directivity measurements. The theoretical models are in a stationary medium which is decidedly not the case for jet exhausts from high speed aircraft. Further, the jet structure changes with distance from the exhaust plane, so the characteristic scales change with space. Despite these severe limitations, it is possible to learn some things

about the sound from a high speed flow exhausting from a nozzle. This is another example in which the characteristic scales are a function of position.

Figure 5-5 shows a shadowgraph of a turbulent jet clearly showing the radiated sound field. The figure shows that the major sound sources are not far from the nozzle exit, but gives little information about the frequency spectrum or speed dependence. To learn more, consider the flow from a circular nozzle; it has three regions as shown in Figure 5-6.

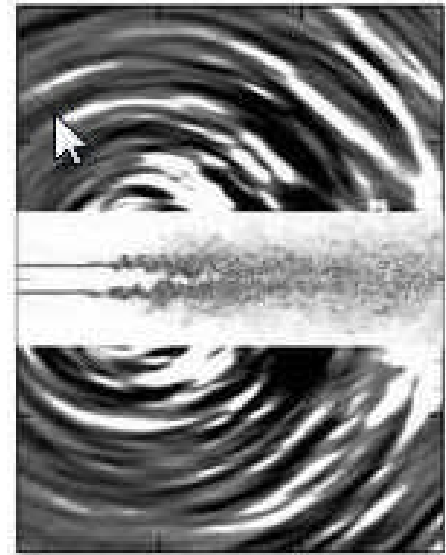


Fig. 5-5. A shadowgraph of jet flow showing the sound field.

### 5.5.1.1 Core Region

The central area of the exit flow may or may not be turbulent, but most importantly the boundary layer will be highly turbulent. Upon exit, that boundary layer grows until the central area consumed. The outer edge of the boundary layer slowly increases radially while the inner edge radius decreases until the central region disappears in about four nozzle diameters. This disappearance is the end of the *core* region. The principle characteristic of this region is that the velocity profile of the mean flow has a flat central contour equal to the exit velocity. For this region, the characteristic length is the thickness of the boundary layer which is an almost linear function of distance from the exit. The characteristic speed is the speed of the central core.

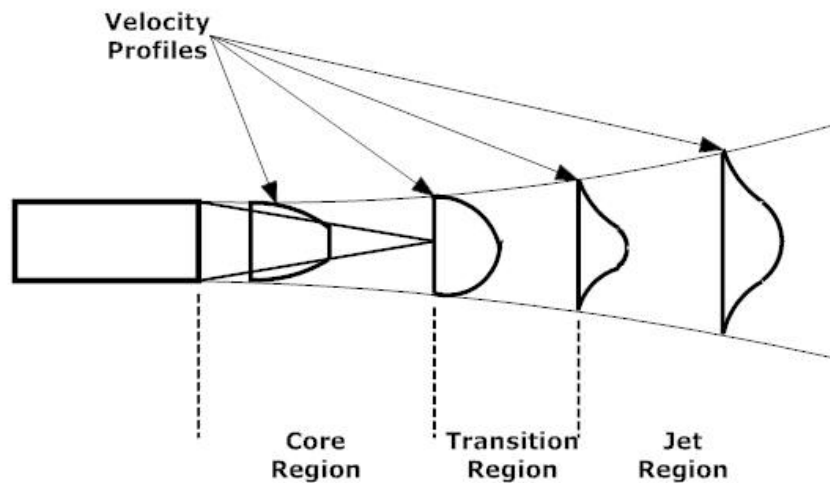


Fig. 5-6. The velocity profiles of a high speed jet.

Consider that the turbulent region is composed of several annular sections, each composed of quadrupole sources. Since the volume of the annular region grows with downstream direction, the size of turbulent eddies must grow and the frequency characteristic of them must lessen. Consider that the core region exists for four diameters then the following approximate relationships on the right apply. The initial boundary layer  $\delta_0$  is that formed within the exhaust pipe whose diameter is  $D$ . The variable  $x$  runs from zero to  $4D$ . The cross sectional area of the radiating turbulence is an annular region

$$Area = \pi\delta(D - \delta)$$

$$\delta = \delta_0 + \left(\frac{D}{2} - \delta_0\right)\frac{x}{4D}$$

that is small at initiation and encompasses the entire jet at the end of the core region. A local volume is defined as the local area times an increment of  $x$ . The radiation is from turbulent eddies of a specific size so that the volume is occupied by a finite number of quadrupole radiators. Eddies increase in size directly with the local volume so they occupy a larger fraction of total local volume as the boundary layer grows. The eddies are presumed to be uncorrelated in each local volume so their powers are mean square additive. Eqs. 5-11 is used to calculate the sound power of each local volume (annular section) and the volumes are summed as independent radiators.

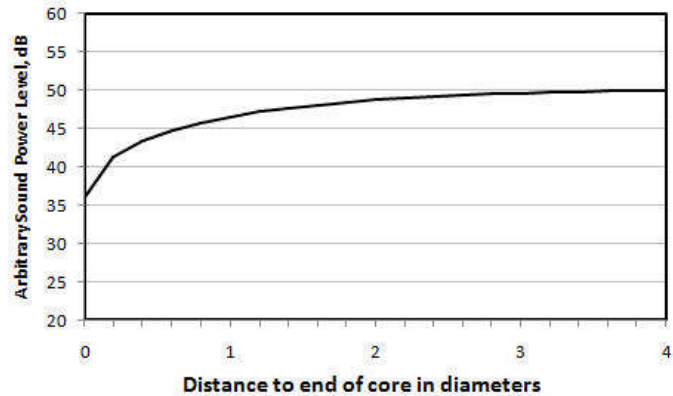


Fig. 5-7. The relative sound power axially in the core region.

An example calculation was done for a nozzle diameter of two feet and exit velocity of 500 ft/sec. Twenty local volumes were summed in the core region to provide relative overall levels. The results, shown in Figure 5-7, are of arbitrary level intended to show the relative contributions to output along the core region. The initial level is the lowest since the annular radiating volume is extremely small relative to downstream volumes. The level rapidly approaches a constant level with distance, suggesting that the entire core region participates significantly in the sound output.

If similarity holds, the Strouhal number is relatively constant over the core distance. The characteristic length is that of the growing boundary layer and the characteristic speed is approximately that of the central core. The maximum frequency of each local volume decreases with distance along the core. The relative spectra of each of the twenty volumes were summed and the resultant one-third octave band spectrum is shown in Figure 5-8. The spectrum contour was that of a haystack spectrum with 6 dB/octave slopes on each side of the maximum. Close to the orifice, the output has higher frequencies, but a lower level. The output further downstream has lower frequencies but a higher level so it masks the high frequency contribution. Surprisingly, for such a simple use of dynamic similarity, measurements of aircraft passes, show spectra that have a maximum near that shown in the figure with similar spectrum contours.

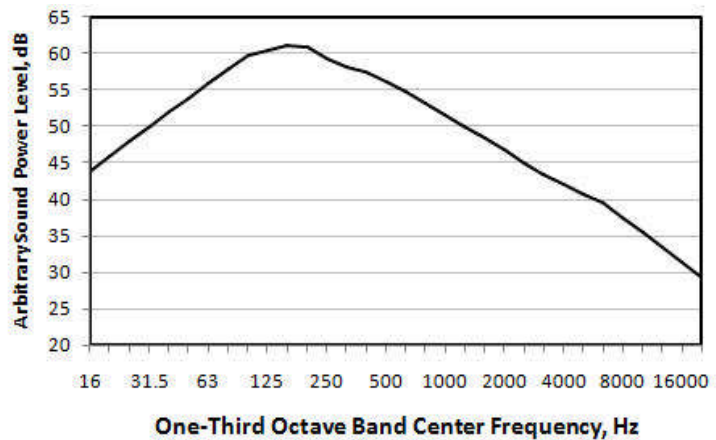


Fig. 5-8. The relative sound power spectrum from the turbulent shear layer in the core region.

**Key Point:** The core region is a large contributor to sound power. This is supported by the shadow graph of Figure 5-5.

### 5.5.1.2 Transition Region

The velocity profile at the end of the core region is similar to that shown in Figure 5-6. The curvature of the profile changes in the transition region. It is more difficult to analyze this region, except to know it must patch together the two regions around it. The characteristic length and speed are difficult to define here.

### 5.5.1.3 Fully Developed Region

The velocity profile for fully developed jet flows is similar to that shown in Figure 5-6. The width of the jet increases, and the centerline velocity decreases with distance from the core region. This region is the only example in this monograph where both of the characteristic scales vary both with downstream distance and lateral distance. Data from measurements suggest a lateral profile similar to the  $U_c \operatorname{sech}(w)$  function where  $w$  is the width (a function of axial distance), and the decay of  $U_c$  is linear with distance. To avoid getting into mathematics more appropriate to research, the lateral profile was subdivided into nine annular regions, much like a multi-tiered cake. The nine annular regions were calculated for positions from  $5 < x/D < 8$  with increments of  $x/d=0.4$ . Essentially, the model was a multi-dimensional summation. Again, without data on eddy intensities or sizes, the scaling rules were used to create the figures below.

Figure 5-9 shows the trend of sound power laterally at  $x/D=5$ . The transition region was set between  $4 < x/D < 5$ . It is clear that since characteristic speed decays rapidly with lateral distance, sound production also falls off significantly. This estimate is based on similar eddy intensities at every lateral position, which is not likely to be correct, since shear on the axis is less. However, the turbulence in the central area along the axis is likely to be the major source of sound at any axial position.

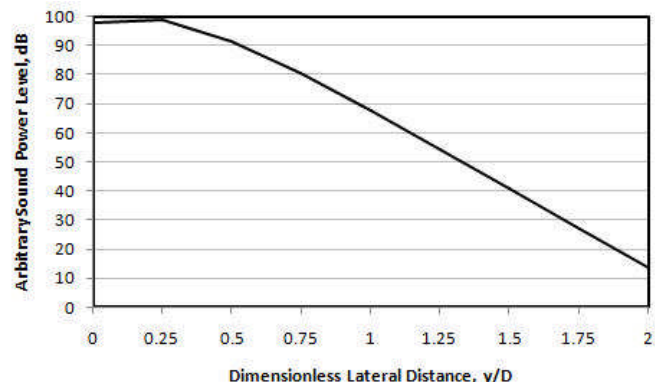


Fig. 5-9. The estimated sound power level contour laterally at  $x/D=5$  in the jet region.

Figure 5-10 shows the trend of sound power in the axial direction, starting at five diameters downstream just at the end of the transition region. The decay is about 18 dB/doubling of distance. The central area grows with distance, as does eddy size, but the speed dependence determines the sound power.

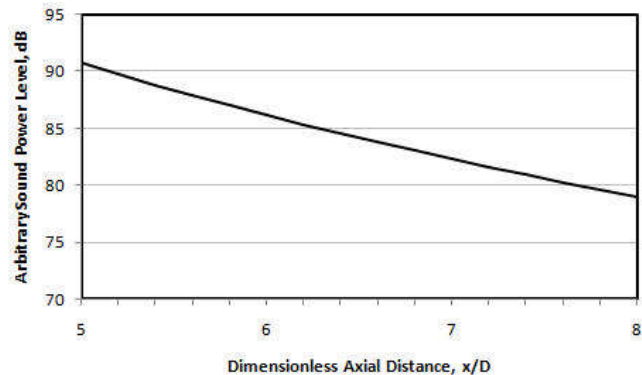


Fig. 5-10. The estimated sound power level contour axially in the jet region.

**Key Points:** This section was not intended to provide a detailed analysis of the sound generated by a subsonic circular jet; that has been the subject of much research. Were any of the magnitudes accurate? No. That kind of information must be determined by detailed theory and experiment. It might be noted that several ad hoc approximations as to eddy size and boundary layer growth were needed, but knowledge of the local characteristic

scales and the quadrupole power law overcomes these limitations. Considerations of directivity were omitted. Not only are the stresses randomly oriented, but velocities are sufficiently high that the sound is redirected by velocity and temperature gradients.

If the thrust is kept constant, the exit velocity is halved when the diameter of the jet is doubled. One-half velocity implies a  $24 \text{ dB}$  reduction in sound emission! Early noise reduction methods attempted to change the flow structure by corrugating the outer edge of the exhaust nozzle to mix the exterior flow with the engine flow. Unfortunately, drag was increased and performance was reduced. Current methods use high-bypass turbofans with greater thrust, fuel efficiency, reduced exit speed and reduced sound generation.

**Key Points:** The purpose was to show how a knowledge framework can be built around the sound radiated by jets with very few tools. In particular, it is known that the sound of high speed jets is quadrupole in nature, and the overall velocity profiles are known. With these two pieces of information, along with scaling rules, it was possible to develop a simple, but reasonable, framework for where the sound was most likely to be emitted. Unlike earlier chapters, this was accomplished by letting the characteristic variables be *functions of space*.

### 5.5.2 Supersonic Circular Jets (Screech Tone)

Because circular jets can radiate in several modes, this section supplements that in {4.10.7}. When a jet emerging into ambient medium has a pressure ratio greater than the critical, the flow becomes supersonic on exit. Details of the concept are given in {4.10.6} and there the rectangular jet shock cells had asymmetric distortions. Here the jet is circular and the instability results in either symmetric or helical distortions of the shock cells. The symmetric distortion occurs at Mach numbers less than 1.25 and the apparent source is near five cells downstream. The helical distortion occurs at greater Mach numbers and occurs near three cells downstream (Are we dealing with a version of the vortex whistle? {4.10.4}). Considering an analogy to the basic source types, in the rectangular jet the center of mass of the cells oscillate laterally giving rise to a dipole-like sound field. In the circular jet with symmetric distortions the volume of the cells vary giving rise to a monopole-like sound field. In the circular jet with helical distortions, the sound field is more like that of a rotating dipole source. A simple equation for the Strouhal number of the screech is

$$St = \frac{fL}{c_0} = \frac{0.7}{u + c_0}$$

The characteristic length  $L$  is the cell length, and the characteristic speed is that of sound. Considering that both speeds are almost equal, a Strouhal number of 0.35 results. Some experimental data have indicated an almost identical value for a Strouhal number based on the orifice diameter as the characteristic length and jet exit speed as the characteristic speed, suggesting the close relationship between the variables.

**Key Points:** Assigning characteristic variables can be difficult. The flow leaving the nozzle will be sonic, expanding to supersonic in the area critical for sound generation, but since one is dependent on the other, the nozzle speed is a reasonable characteristic speed. Since it is eddies passing through the shock cells that cause the disturbance, it would seem that the characteristic length would be cell spacing. As with all free jet flows, the characteristic variables are a function of position in the jet.